Surface Science 95 (1980) 571–586

SURFACE CHEMISTRY OF THE METAL–HALOGEN INTERFACE: BROMINE CHEMISORPTION AND RELATED STUDIES ON VANADIUM (100)

P.W. DAVIES * and R.M. LAMBERT
Department of Physical Chemistry, University of Cambridge, Cambridge, CB2 1EP, England

Received 7 December 1979; accepted for publication 1 February 1980

Bromine adsorbs dissociatively on the V(100) – (5 × 1) reconstructed surface at 300 K with a constant sticking probability of 1.0. A chemisorbed overlayer of atoms is formed which, at $\theta = 0.5$, culminates in a c(2 × 2) structure. For $0.5 < \theta < 0.75$, epitaxial growth of the first layer of VBr_2(331) begins, and a (6 × 4) structure appears. For $\theta > 0.75$ multilayer growth of VBr_2 proceeds, the Br_2 sticking probability remains unchanged, and at 300 K the system effectively saturates at $\theta \sim 4$. The Br^+, V^+, and VBr^+ desorption spectra show three distinct maxima which characterise each of the above three phases of evolution of the V–Br interface. For $\theta <$ 0.5 only Br atoms are desorbed. In the regime $0.5 < \theta < 0.75$ first-layer VBr_2 evaporation commences. For $\theta > 0.75$ a third peak appears and corresponds to evaporation of VBr_2 from the multilayer system. In this final stage fractional order kinetics are exhibited which reflect the increasing Madelung energy of the growing VBr_2 crystal: the activation energy to desorption converges rapidly on a value which is equal to the sublimation enthalpy of bulk VBr_2. In the presence of Na, adsorbed NaBr is formed in preference to VBr_2: when the NaBr coverage reaches a full monolayer it renders the vanadium surface impervious to corrosion by Br_2. Oxygen adsorption on the Na dosed surface at 300 K leads to very efficient loss of alkali, possibly by immediate evaporation of an exothermically formed sodium oxide. The energetics of the V–Br_2 system are considered in detail, and a model is developed which fits all the thermal, structural and kinetic data.

1. Introduction

Studies of halogen adsorption under UHV conditions are relatively rare (see for example refs. [1–7] and references therein) and it is true to say that no general trends have emerged that are directly relevant to this work. On the other hand, the adsorption of alkalis on metal surfaces has been rather more extensively researched. In particular, the theory of the alkali–metal bond [8,9] and the influence of alkali adsorption on surface work functions [10,11] appear to be well understood.

Accordingly, in this work the adsorptive properties of bromine, sodium and

* Present address: Department of Chemistry, University of California, Berkeley, California 94720, USA.

oxygen on the V(100) surface have been studied both as single adsorbate systems and, to a lesser extent, as mixed adsorbate systems (viz. Na/O_2; Na/Br) with most attention being focussed on the V–Br system. Oxygen adsorption on vanadium has been investigated by other workers [12–14] and is therefore discussed here only in the context of the mixed adsorbate systems. A limited amount of work was also performed using a (100) faceted V(111) specimen [15]. Its behaviour was found to be virtually identical to that of the V(100) specimen, except in that no surface structural information could be obtained. Therefore, the results presented are discussed mainly in terms of the V(100) specimen, with references being made to the V(111) specimen at points where specific differences in behaviour were observed.

2. Experimental

Both specimens were cut from the same single crystal rod (99.99+% purity, Metals Research Ltd.) after orientation, slicing and polishing the final dimensions were ~11 mm diameter × 0.8 mm thick. These specimens were attached to 3 mm diameter Ta support rods by means of 0.25 mm diameter Ta wires, and carried Pt/Pt–10% Rh thermocouples. The experimental geometry was such that in desorption experiments (i) the mass spectrometer ion source subtended a large solid angle at the specimen: this gave a high sensitivity to desorbing reactive species; (ii) desorption from the specimen supports did not cause interference problems.

Bromine and sodium dosing were carried out using a solid state electrolytic cell and zeolite based ion source respectively. Both these devices have already been described [2]. The amount of bromine incident at the crystal surface is directly related to the *total charge* passed through the cell during electrolysis, and it is this value which is quoted alongside the desorption traces. As will be discussed below, both LEED and thermal desorption data indicated that a surface coverage of about $\frac{1}{2}$ of a mono-layer of bromine atoms was achieved after an electrolysing charge of 1200 μC. If a constant sticking probability of unity is assumed, it may be estimated that a charge of 1200 μC yields a total bromine flux of 0.25×10^{15} molecules cm^{-2} at the crystal surface – i.e. about 8% of the bromine produced by the cell is incident at the vanadium surface. This compares favourably with a value of 9% which may be calculated from the known dimensions and geometry of the cell collimator tube. In the results which follow, approximate values of θ are stated along with the exact Br_2 doses. $\theta = 1$ is taken as a number density of Br *atoms* equal to that of the metal atoms in a V(100) plane.

3. Bromine chemisorption: results and discussion

It is difficult to prepare a clean vanadium surface: the most troublesome impurity was bulk sulphur which could only be removed by about 200 h Ne^+ bombard-

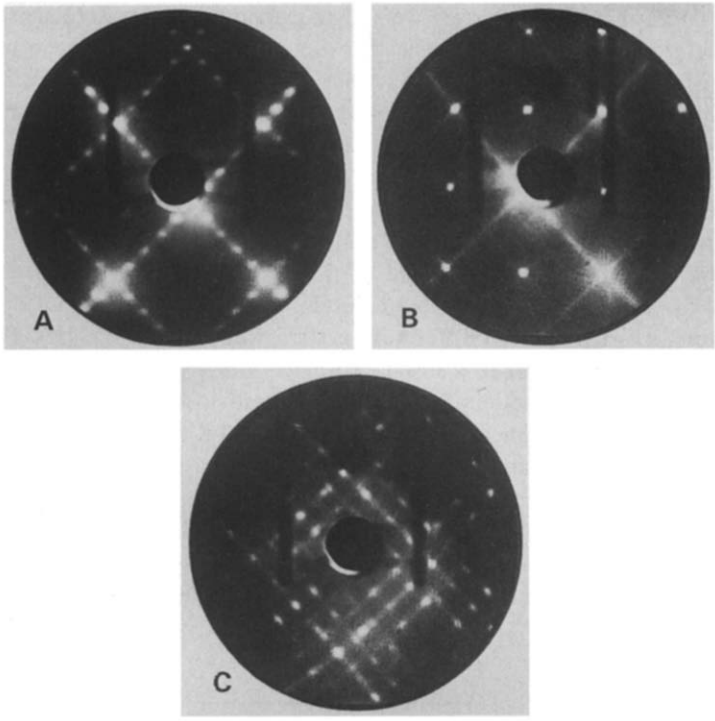

Fig. 1. LEED patterns: (A) V(100)-(5 × 1) reconstructed clean surface, 77 V; (B) c(2 × 2) bromine overlayer structure, 62 V; (C) V(100)/$VBr_2(3\bar{3}1)$-(6 × 4) structure, 50 V.

ment at 800 K. The clean surface is reconstructed and is characterised by a (5 × 1) LEED pattern at 300 K (fig. 1A). This fact has not been recognised nor reported previously. The (5 × 1) structure undergoes a reversible phase transition to the (1 × 1) structure at about 630 K. This behaviour has been investigated in detail, and we have presented elsewhere [16] a full structure analysis of the (5 × 1) reconstructed surface using the LEED intensity data. Briefly, the (5 × 1) structure is thought to consist of a single slightly rumpled bcc (110) layer lying on top of the normal bulk bcc (100) planes: the structure is therefore reminiscent of the (5 × 20) reconstruction which occurs at the (100) surfaces of the fcc metals Au and Pt. It does however appear to be unique among the bcc metals. Earlier workers may very well have failed to observe the (5 × 1) structure because of the extreme difficulty of sulphur removal; sulphur stabilises a (1 × 1) surface structure.

LEED observations indicated that the adsorption of Br_2 on the clean V(100)-(5 × 1) reconstructed surface at 300 K led initially to the disappearance of the fifth-order maxima, with a well-formed (1 × 1) pattern being observed after Br_2 exposures of about 600 μC ($\theta \sim 0.25$). LEED patterns subsequently obtained from

the V(100)/Br_2 adsorption system were characteristic of a four-fold substrate surface, thus providing further evidence that Br_2 adsorption did induce a real structural transformation in the vanadium surface. Further exposure to Br_2 at 300 K led to continued uptake beyond the monolayer stage (see below) with attenuation of the integral-order beams and a simultaneous increase in the LEED-background intensity, until, after about 600 μC ($\theta \sim 2.5$) exposure, all diffraction features were completely extinguished. At room temperatures, no ordered phases could be formed up to Br_2 exposures of >10000 μC ($\theta > 4$).

However, if, after a Br_2 exposure of 1200 μC ($\theta \sim 0.5$), the specimen was annealed for a short period at about 700 K, and subsequently cooled to room temperature, a sharp c(2 X 2) diffraction pattern was formed (fig. 1B). This structure is taken to correspond to a surface coverage of $\theta = 0.5$, and, therefore, forms the basis of the coverage calibration. Similar, but rather more diffuse patterns were observed subsequent to annealing the specimen at 700 K after lower Br_2 exposures. The c(2 X 2) diffraction pattern was stable up to temperatures of about 1100 K.

A rather more complex pattern was observed after exposing the crystal to between about 1800 μC ($\theta \sim 0.75$) and about 10000 μC ($\theta \sim 4$) of Br_2 and subsequently annealing at about 700 K. A photograph of this pattern, which is indexed in terms of two perpendicular domains of a (6 X 4) coincidence overlayer structure,

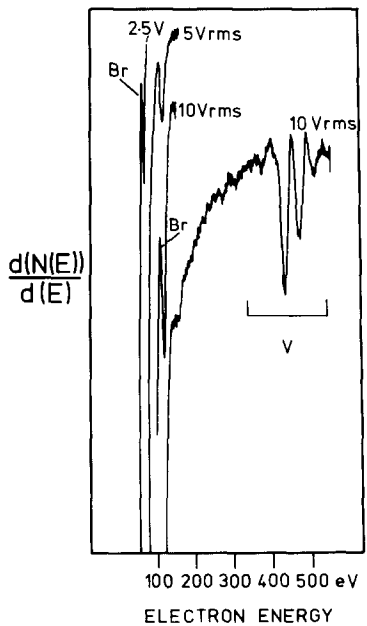

Fig. 2. Auger spectrum of bromine saturated surface: primary beam 8 μA at 2000 V.

is presented in fig. 1C. Annealing the crystal at 700 K, after intermediate Br_2 exposures of between about 1200 μC ($\theta \sim 0.5$) and 1800 μC ($\theta \sim 0.75$), led to the formation of a pattern which was a superposition of the diffraction maxima from both the c(2 X 2) and (6 X 4) LEED patterns. The (6 X 4) pattern was transformed into a c(2 X 2) pattern by heating the crystal to about 1000 K.

Both the 105 V and the 85 V Br transitions could be clearly resolved in the Auger spectrum of a Br dosed V(100) surface. The intensities of these transitions increased smoothly with increasing Br exposure, reaching a saturation value after about 10000 μC ($\theta \sim 4$). An Auger spectrum obtained from the bromine saturated V(100) surface is shown in fig. 2.

AES studies also revealed that the surface bromine concentration concurrent with the formation of a c(2 X 2) LEED pattern after about 1200 μC exposure, was identical to that of the c(2 X 2) LEED pattern formed by heating the (6 X 4) structure at about 1000 K.

Thermal desorption studies detected product desorption at amu 79 (Br^+), amu 51 (V^+) and amu 130 (VBr^+). Other possible desorption products, e.g. amu 209

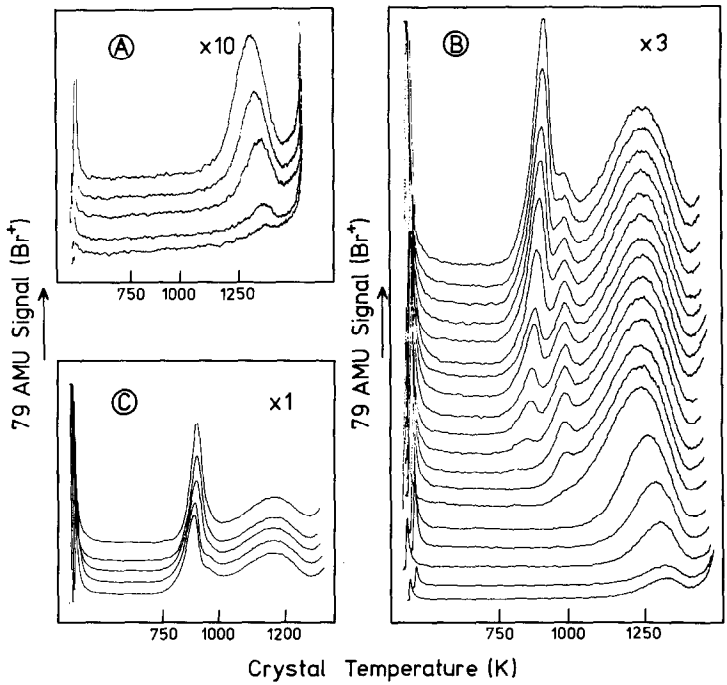

Fig. 3. Br^+ desorption spectra, heating rate 70 K s^{-1}. Br_2 doses in molecules $cm^{-2} \times 10^{-14}$ as follows: (A) 0.1, 0.4, 1.2, 1.9, 3.1; (B) 0.2, 0.4, 1.2, 1.9, 2.5, 3.1, 3.7, 4.1, 4.6, 5.0, 5.4, 5.8, 6.7, 7.1, 7.5, 7.9, 8.3, 8.7, 9.1; (C) 8.3, 10.0, 11.4, 14.6.

(VBr_2^+), amu 288 (VBr_3^+) etc., could not be directly observed due to the limited mass range of the quadrupole mass spectrometer used during these investigations.

Amu 79 desorption traces are reproduced in fig. 3. At low exposures (<1200 μC) a single, rather broad, desorption peak was detected. The peak was symmetric about the position of its coverage-dependent maximum, which was found to decrease from about 1375 K after a Br exposure of 50 μC ($\theta \sim 0.02$), to about 1240 K after a Br exposure of 1200 ($\theta \sim 0.5$), at which point saturation occurred. This behaviour is characteristic of second-order desorption kinetics. However, since only bromine atom desorption could be detected (with no desorption occurring at amu 158 (Br_2^+)), it is probable that the desorption process obeys first-order kinetics, modified by the presence of strong repulsive lateral-interactions between atoms in the adsorbed phase. Application of the first-order desorption equation, with a pre-factor of 10^{13} s^{-1}, enables approximate activation energies to desorption of 334 kJ $mole^{-1}$ at low coverage decreasing to 309 kJ $mole^{-1}$ at $\theta = 0.5$, to be evaluated.

Above 1200 μC exposure a second, lower temperature, desorption state developed and rapidly reached saturation at about 1800 μC ($\theta \sim 0.75$) Br_2 exposure. This peak was quite sharp, and displayed an almost coverage-independent maximum at 1000 K. Assuming first-order desorption kinetics, an activation energy to desorption of about 240 kJ $mole^{-1}$ is evaluated.

A third, and final, desorption state centred at about 900 K was observed at exposures >1800 μC ($\theta \sim 0.75$). This peak was asymmetric in form about its peak maximum, which moved to slightly higher temperatures at increased Br coverages: a behaviour which is suggestive of zero- or fractional-order kinetics. Saturation was reached after about 10000 μC ($\theta \sim 4$), at which point this peak formed the major part of the total desorption profile. Activation energies to desorption for this latter state were derived from the slopes of graphs of ln (signal) versus $1/T$, which were constructed by using values obtained from the leading edges of the desorption traces. The derived activation energies increased smoothly from about 90 kJ $mole^{-1}$ for the 2200 μC desorption trace, to about 205 kJ $mole^{-1}$ for the 3600 μC desorption trace, after which point the activation energies remained constant to within 5 kJ $mole^{-1}$.

For conciseness, the three desorption states will be referred to, in order of increasing desorption energies, as the α, β and γ states. Also present in the amu 79 desorption traces were a sharp peak at about 300 K, and a high-temperature shoulder; these were experimental artifacts arising from the desorption of bromine atoms from, respectively, the Ta heating wires, and the Ta support rods. This assignment is based on a number of control experiments: it is confirmed by inspecting the V^+ and VBr^+ spectra in which neither of these features arises.

Amu 51 (V^+) desorption spectra are shown in fig. 4A. The high-temperature γ-state is completely absent, but both the α- and the β-states are observed, and are identical in both shape and relative intensity to the corresponding peaks in the amu 79 desorption spectra. It may be concluded, therefore, that both these latter states are associated with the desorption of vanadium bromide species of identical stoi-

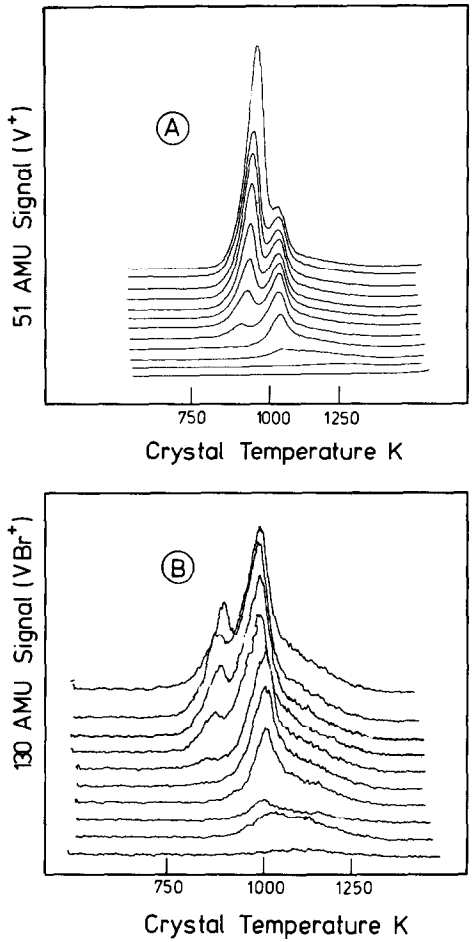

Fig. 4. (A) V^+ desorption spectra; (B) VBr^+ desorption spectra. Heating rate 70 K s^{-1}; Br_2 doses in molecules $cm^{-2} \times 10^{-14}$ as follows: (A) 0.4, 1.9, 2.5, 3.1, 3.7, 4.6, 4.8, 5.0, 5.4, 5.8, 6.7, 7.5; (B) 1.9, 2.1, 2.3, 2.5, 2.7, 2.9, 3.1, 3.3, 3.5, 3.7.

chiometry, although the precise nature of this species cannot be determined from the desorption data alone. The amu 51 desorption spectra also reveal that the β-state has a high-temperature tail which extends up to about 1320 K: a feature which was masked by the presence of the γ-state in the amu 79 spectra.

Amu 130 (VBr^+) desorption spectra (fig. 4B) display a form which is identical to that shown by the amu 51 spectra. As was discussed previously, experimental limitations prevented the direct observation of higher molecular weight species. However, desorption signals corresponding to the doubly charged VBr_2^{2+} ion (m/e =

104.5) were detected at temperatures corresponding to the α- and the β-desorption states, but, unfortunately, these signals were far too weak to be quantitatively useful. By using the thermal desorption yields as a measure of the total bromine uptake, one concludes that the sticking probability of Br_2 is essentially constant, and in particular that it remains unchanged as the system proceeds beyond $\theta \sim 1.0$. An absolute value for this sticking probability may be estimated by noting the total Br_2 dose required to generate the most perfect c(2 × 2) structure to which we assign the value $\theta = 0.5$. The result is: sticking probability = 1.0.

Work function measurements revealed that $\Delta\phi$ increased smoothly with bromine coverage, reaching a maximum value of +1.05 V after about 3000 μC ($\theta \sim 1.25$).

Dependent upon the total amount of bromine present in the surface regions, the V(100)/Br_2 adsorption system may display three markedly different types of behaviour:

At bromine coverages of $\theta < 0.5$, both the desorption and LEED data suggest that bromine adsorbs dissociatively, and exists on the crystal surface as an ordered array of chemisorbed bromine atoms. This array may be identified with the γ-desorption state. The derived activation energies to desorption from this state (310–334 kJ $mole^{-1}$) can therefore be equated to the vanadium–Br interaction energy. For comparison, the V–Br bond energy in VBr_2 is about 450 kJ $mole^{-1}$ [17].

A rather more complex picture emerges at higher coverages. In the regime $0.5 < \theta < 0.75$, LEED observations reveal the formation of islands of a (6 × 4) structure in the V(100)–Br c(2 × 2) structure, whilst the desorption data indicate that a vanadium bromide species is produced by evaporation of the adlayer (the β-desorption state).

Structural models for the (6 × 4) diffraction pattern were considered in the context of the epitaxial growth of a bulk vanadium bromide on the vanadium crystal surface. A pre-existing computer program was employed to search all the crystal planes in the stable bulk vanadium bromides (VBr_2 and VBr_3) for suitable coincidences with the V(100) plane. A unique solution, was obtained which requires only 3.5% contraction of the halide lattice along $\{3\bar{1}2\}$; the $(3\bar{3}1)$ plane of VBr_2 ($Ca(OH)_2$ structure, $a = b = 3.786$ Å, $c = 6.1803$ Å and u is undetermined [18]) was found to generate the required mesh when placed on the V(100) surface. A schematic diagram of this solution appears in fig. 5. It may be observed that this solution is physically reasonable, since the V^{2+} and Br^- ions are virtually co-planar – if a value for $u = \frac{1}{3}$ is assumed, the Br^- ions will be alternately positioned at 0.17 Å above and below the plane containing the V^{2+} ions.

The unit cell of the $(3\bar{3}1)$ plane in VBr_2 has an area of 72 $Å^2$ and contains two Br^- ions. Whereas, in the V(100)–Br c(2 × 2) structure each bromine atom occupies 18 $Å^2$. A monolayer of the $(3\bar{3}1)$ plane of VBr_2 would therefore contain exactly one half of the amount of bromine present in the c(2 × 2) structure. This is entirely consistent with the observed Br_2 doses which were required to form the c(2 × 2) and (6 × 4) structures (1200 and 1800 μC respectively) and the constant Br_2 stick-

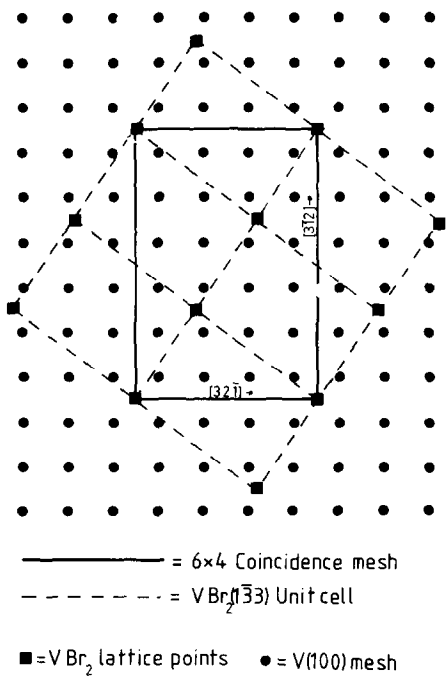

Fig. 5. Proposed structure for (6 × 4) phase: (■) VBr_2 lattice points, (●) V(100) mesh points.

ing probability of unity. Recalling the TDS data, it is evident, therefore, that the β-desorption state should be identified with the growth of a single layer on the (3$\bar{3}$1) plane of VBr_2 on top of the V(100)–Br c(2 × 2) structure.

Investigations into the properties of bulk VBr_2 [17] have shown that after sublimation only the dibromide is present in the gas phase. It is therefore assumed, although only an indication is available from the present work, that desorption from the β-state (and, indeed, the α-state) occurs solely in the form of VBr_2 molecules, with the detected amu 51 (V^+) and amu 130 (VBr^+) signals resulting from fragmentation processes occurring within the mass spectrometer. (VBr_2^+ beyond accessible mass range, weak VBr_2^{2+} signals observed).

The activation energy to desorption from the β-state was found to be about 240 kJ $mole^{-1}$; this value may depend both on the interactions between the VBr_2 units within the (3$\bar{3}$1) plane, and on the interactions between the VBr_2 units and the vanadium substrate. This latter term will be sensitive to the topology of the metal surface. During desorption experiments from the bromine dosed faceted V(111) surface it was found that, although desorption from the α- and β-states occurred at temperatures identical to those observed during desorption from the V(100) surface, the β-state occured at about 50 K lower in temperature, being detected only as

a high-temperature shoulder on the α-desorption peak. This may be due to the fact that during the growth of the first layer of VBr_2 on the faceted V(111) surface a less satisfactory fit to the substrate geometry was achieved than was found to be possible during the growth of VBr_2 on the V(100) surface.

At coverages $\theta > 0.75$, the development of the (6 × 4) diffraction pattern on the V(100) surface is complete, and a second vanadium bromide desorption state (the α-state) appears in the TDS spectra. It is proposed that this state arises from the growth of subsequent layers of the VBr_2 ($3\bar{3}1$) plane. The activation energy to desorption from this state was found to rise from about 90 kJ mole^{-1} at its inception, to about 205 kJ mole^{-1} after a total bromine exposure of 3600 μC (which, assuming unit sticking probability, is equivalent to the growth of four crystal planes of VBr_2). These variations may be attributed to the increasing mutual electrostatic attractions between individual molecular units which accompany the growth of an ionic crystal. It may be seen that the activation energy to desorption at high coverages approximates to the sublimation energy for bulk VBr_2 of 213 kJ mole^{-1} [19]. An alternative growth mechanism for the α-state may be considered in terms of the formation of pyramids of VBr_2 on top of the first monolayer of the $VBr_2(3\bar{3}1)$ plane. However, it is to be expected that the *initial* activation energies to desorption from such a state would remain roughly constant, and also rather low, since it would always contain a large number of low-coordinated, i.e. weakly bound, VBr_2 units.

3.1. Energetics

The energetic feasibility of the various adsorption and desorption processes which were discussed above will now be considered. For conciseness the following terminology is adopted: $E_d(\alpha)$, $E_d(\beta)$ and $E_d(\gamma)$ will refer to the activation energies to desorption from the α-, the β-, and the γ-states respectively, whilst $E_{ad}(\alpha)$, $E_{ad}(\beta)$ and $E_{ad}(\gamma)$ will refer to the energies released during adsorption into those respective states; $E_{\gamma\to\beta}$ will refer to the activation energy required to transform the γ-state into the β-state. Fig. 6 illustrates these terms and may prove helpful in clarifying the arguments presented below. All the thermodynamic quantities used have been obtained from either ref. [19] or the present thermal desorption studies.

$E_{ad}(\gamma)$ may be derived from the following reaction sequence:

$$2\,V_{(s)} + Br_{2(g)} \xrightarrow{193\ \text{kJ mole}^{-1}} 2\,V_{(s)} + 2\,Br_{(g)} \xrightarrow{-2E_d(\gamma)} 2\,V\text{–}Br_{(ad)}\,.$$

Hence

$$E_{ad}(\gamma) = 2E_d(\gamma) - 193\ \text{kJ mole}^{-1}\,.$$

Since $E_d(\gamma)$ was found to vary between 334 kJ mole^{-1} at $\theta \sim 0.02$, to 309 kJ mole^{-1} at $\theta \sim 0.5$, it follows that $E_{ad}(\gamma)$ will vary between 475 kJ mole^{-1} and 425 kJ mol^{-1} in the same coverage regime. It may be noted that the energy released in

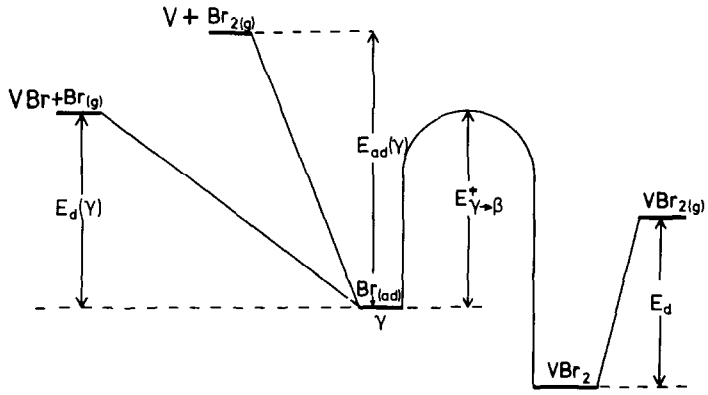

Fig. 6. Energetics of the vanadium–bromine adsorption/desorption system.

forming two V–Br chemisorptive bonds far exceeds the energy required to break the Br–Br bond.

The precise behaviour of $E_{ad}(\gamma)$ at coverages of $\theta > 0.5$ cannot be directly determined from the experimental data. However, it has long been recognised that the energy of adsorption into an array of mutually repulsive particles arranged on a four-fold surface decreases dramatically at coverages around 0.5, since above this coverage particles are forced to occupy nearestneighbour sites [20–22]. The behaviour of the γ-state at coverages of $\theta < 0.5$ indicates that repulsive lateral interactions are present in the adsorbed layer, and therefore it is expected that $E_{ad}(\gamma)$ will decrease in a similar fashion at coverages $\theta \sim 0.5$.

$E_{ad}(\beta)$ may be estimated from the following Born–Haber cycle:

$$\begin{array}{ccc} V_{(g)} + Br_{2(g)} & \xrightarrow{-750\ \text{kJ mol}^{-1}} & VBr_{2(g)} \\ \uparrow \Delta E_{sub}(V) = 512\ \text{kJ mol}^{-1} & & \downarrow E_d(\beta) = 240\ \text{kJ mol}^{-1} \\ V_{(s)} + Br_{2(g)} & \xrightarrow{E_{ad}(\beta)} & VBr_{2(ad)} \end{array}$$

Hence, $E_{ad}(\beta) = -478$ kJ mol^{-1}. This value will be almost independent of the total surface bromine concentration.

The energy to adsorption into the β-state is therefore greater than the energy to adsorption into the γ-state at all surface bromine coverages, and yet, below about 0.5 monolayer desorption occurs exclusively via the γ-state. There are two possible ways for accounting for this:

(1) Adsorption occurs in the β-state, but the adsorbed phase transforms into the γ-state during the desorption sweep, and desorption occurs in the form of bromine atoms. However, an examination of fig. 6 completely rules out this possibility. It

may be seen that the energy required to desorb the β-state in the form of bromine atoms is $668 - E_d(\gamma)$ kJ mol^{-1}, which will always be greater than $E_d(\beta)$.
(2) Adsorption into the β-state is an activated process. Mechanistically, this explanation is reasonable, since adsorption into the β-state will be expected to proceed via dissociative adsorption into the γ-state, followed by an activated atomic rearrangement into the β-state.

If it is assumed that the energy of the activated complex in the transition from the γ- to the β-state is independent of surface bromine coverage, it may be seen from fig. 6 that $E_{\gamma\to\beta}$ becomes a simple function of $E_d(\gamma)$, viz.:

$$E_{\gamma\to\beta} = 2E_d(\gamma) + \text{constant} .$$

Three regimes of behaviour, corresponding to decreasing values of $E_d(\gamma)$, may now be identified.
(1) $E_d(\gamma) < E_{\gamma\to\beta}$ ($\theta < 0.5$). The system will show a simple one-state behaviour, with adsorption and desorption occurring exclusively via the γ-state.
(2) $E_d(\gamma) \sim E_{\gamma\to\beta}$ ($\theta \sim 0.5$). Adsorption will occur exclusively into the γ-state, but desorption may occur directly as bromine atoms, or via the β-state as VBr_2 molecules. The high-temperature tail associated with the β-desorption state in the amu 51 desorption spectra (fig. 4A) is attributed to this latter process.
(3) $E_d(\gamma) > E_{\gamma\to\beta}$ ($\theta > 0.5$). Adsorption occurs directly into the β-state and VBr_2 is the sole desorption product.

At $\theta > 0.75$ the β-adsorption state is full, and, therefore adsorption is forced to proceed via the energetically less favourable α-state.

4. Sodium chemisorption: results and discussion

Sodium was dosed on to the surface by a 3eV Na^+ beam produced by the zeolite source. LEED studies revealed that the adsorption of Na led to the rapid attenuation of both the integral- and fractional-order beams, which, combined with the commensurate increase in background intensity, resulted in the complete extinguishing of all diffraction features at sodium coverages above $\theta \sim 0.4$. Attempts to obtain new ordered phases by adsorbing up to $\theta = 10$, and subsequently annealing at various temperatures, were unsuccessful.

Due to the low excitation cross-section of sodium with 2 keV electrons, only an extremely weak 1000 V Na Auger transition could be detected from a surface containing many monolayers of sodium.

Thermal desorption results from the Na dosed V(100)-(5 × 1) surface are presented in fig. 7. It may be observed that all spectra obtained at $\theta < 1$ consist of two rather broad and overlapping peaks which are centred at about 600 K and about 750 K respectively. It is suggested that the lower temperature peak arises from the desorption of adsorbed sodium, whilst the higher temperature peak results from the desorption of sodium which was absorbed into the subsurface regions during the impact of the hyperthermal sodium ions.

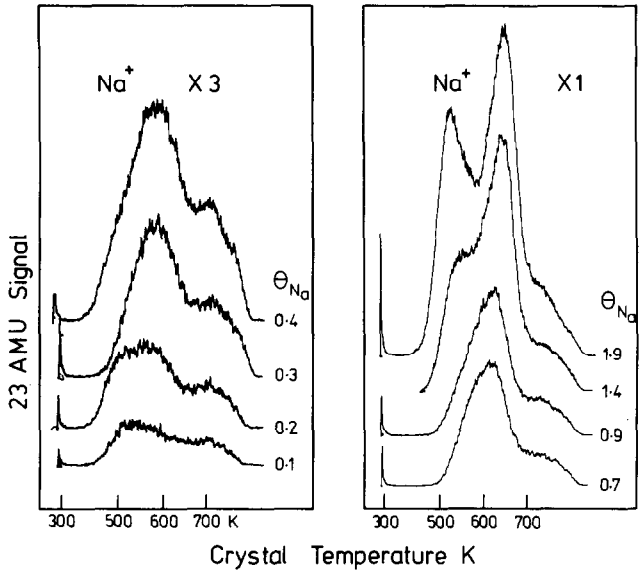

Fig. 7. Thermal desorption spectra from sodium dosed surface. Heating rate 70 K s^{-1}.

For $\theta > 1$, a third, lower temperature peak is observed. The activation energy to desorption from this state was calculated from the slope of ln (signal) versus $1/T$, which was plotted using values obtained from the leading edge of a $\theta = 2.5$ desorption trace. An experimental value of about 91 kJ $mole^{-1}$ was obtained, which may be compared with the bulk sublimation energy for sodium of 89 kJ $mole^{-1}$. This latter state is therefore identified with the desorption of sodium atoms from the second and subsequent atomic layers.

5. Mixed adsorbate systems: results and discussion

5.1. Bromine/sodium

Amu 79 desorption spectra from a V(100) surface containing both Na and Br are presented in fig. 8A. A new low-temperature peak is observed, which parallel amu 102 desorption results indicated was due to the formation of NaBr.

Slight differences in the behaviour of the system were detected, dependent on the order in which the surface was dosed with the alkali and halogen. If bromine was pre-adsorbed exposing the surface to Na^+ ions led to a quantitative, and sequential, depletion of the α-, β-, and the γ-states, together with a corresponding increase in the NaBr desorption peak. However, if sodium was pre-adsorbed, and the crystal

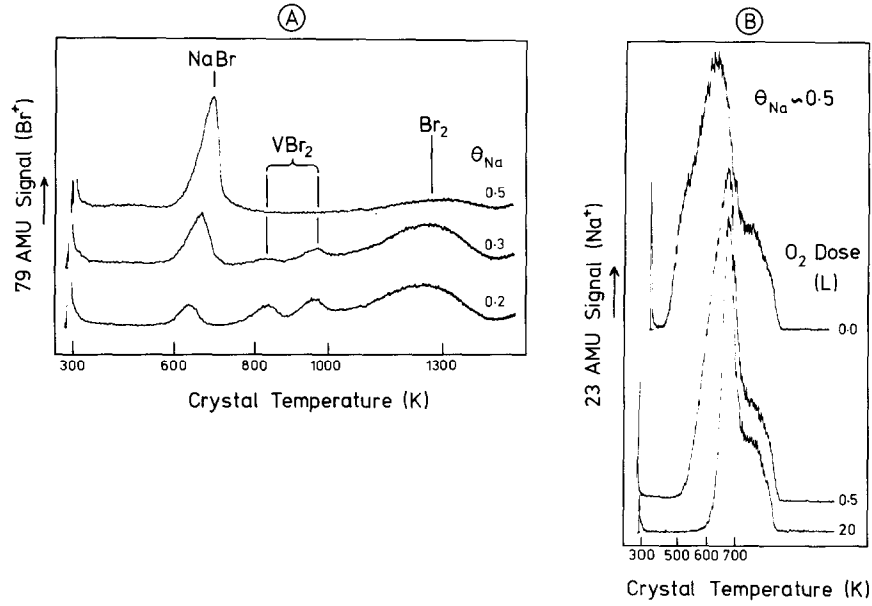

Fig. 8. A: Br^+ following Br_2 saturation of Na pre-dosed surface. B: Na^+ desorption spectra showing effect of subsequent dosing with O_2 at 300 K. Heating rate 70 K s^{-1}.

subsequently exposed to Br_2, desorption spectra indicated that, although the adsorbed sodium was quantitatively converted to NaBr, the subsequent uptake of Br into the α-, β-, and the γ-states was inhibited. The inhibition was complete after initial Na doses of $\theta > 0.5$, and therefore this effect is attributed to the blocking of the vanadium surface by a layer of NaBr. The formation of alkali halide monolayers as a result of alkali and halogen coadsorption on metal surfaces has been established by LEED studies of Na + Br and K + Cl on Ag [2,23].

5.2. *Sodium/oxygen*

As has already been mentioned, the behaviour of oxygen as a single adsorbate on vanadium single-crystal surfaces has been extensively studied by other workere. The adsorption of oxygen on both the V(100) and the V(111) specimens was reinvestigated during the present work, but no novel features were observed. It was found that oxygen adsorbs readily on both surfaces at room temperature, inducing on the V(100) specimen a transformation from the (5 × 1) to the (1 × 1) surface structure. During desorption studies, no oxygen-containing species could be detected, but Auger spectroscopy revealed that the adsorbed oxygen was rapidly removed from the surface regions at crystal temperatures of about 700 K. It was therefore concluded that at this temperature oxygen was rapidly dissolved into the crystal bulk.

The adsorptive properties of oxygen on the Na pre-dosed V(100) surface were also investigated. Auger studies showed that initially no oxygen was adsorbed into the surface regions, but that after certain exposures, which depended upon the surface sodium concentration, oxygen uptake was again rapid.

During thermal desorption from surfaces containing varying amounts of both oxygen and sodium, only amu 23 (Na^+) signals could be detected, with no desorption occurring at any of the other possible mass numbers (amu 16 (O^+), amu 32 (O_2^+), amu 39 (NaO^+), amu 45 (NaO_2^+), amu 62 (Na_2O^+), amu 78 ($Na_2O_2^+$)).

Amu 23 desorption spectra from a surface initially pre-dosed to $\theta = 0.5$ with Na and subsequently exposed to various amounts of oxygen are presented in fig. 8B. It may be seen that, although the portion of the spectra above 710 K are unaffected by exposure to oxygen, the low temperature portion is progressively removed by increasing oxygen exposures. Similar behaviour was observed at all other sodium exposures.

The apparent initial activation energies to desorption for sodium after varying oxygen exposures was derived from the leading edges of the spectra in fig. 8B. It was found that this energy increased rapidly from about 90 kJ $mole^{-1}$ in the absence of oxygen and reached a saturation value of about 190 kJ $mole^{-1}$ after about 5 L O_2 exposure.

A tentative explanation for these observations is offered. Exposure of the sodium dosed V(100) surface to oxygen may result in the formation of a sodium oxide species, which, it appears, desorbs into the gas phase immediately after its formation. Evidently the energetics of such a process will depend upon the strength of the Na–vanadium chemisorptive bond, and the reaction will cease above a certain bond energy, which the desorption data indicate is about 190 kJ mol^{-1}.

6. Summary

(1) Bromine chemisorbs on V(100)-(5 × 1) at 300 K with an essentially constant sticking probability of unity. At $\theta = 0.5$ a c(2 × 2) structure reaches its maximum degree of perfection, and is identified as a chemisorbed overlayer.

(2) For larger bromine uptakes, layer by layer growth of vanadium bromide begins, and the sticking probability remains unchanged as the system enters the multilayer regime. LEED shows the development of a (6 × 4) structure which corresponds to epitaxial growth of VBr_2.

(3) The desorption spectra show three distinct maxima which exhibit very different kinetic characteristics. At the lowest coverages (c(2 × 2) overlayer regime) the only desorption product is Br *atoms*. At intermediate coverages, for which LEED shows that the growth of the first layer of VBr_2 has begun, a new peak due to vanadium bromide evaporation appears. At the highest coverages yet a third peak appears, again due to vanadium bromide evaporation, and exhibiting fractional-order desorption kinetics. This is ascribed to multilayer growth of VBr_2, and the

observed activation energy to desorption converges rapidly to a value equal to the sublimation energy of bulk VBr_2. The kinetic behaviour in this regime reflects the steadily increasing Madelung energy of the system as the VBr_2 crystal grows.

(4) The energetics of the V–Br_2 system are considered in detail and shown to be in accord with all the thermal, kinetic and structural data, and with our proposed model.

(5) Co-adsorption of Na and Br leads to the formation of NaBr which, when present as a single layer, renders the vanadium surface impervious to further corrosion by bromine.

(6) However, adsorption of oxygen on the Na dosed surface appears to have a very different outcome. Much of the alkali is removed at 300 K, possibly by immediate evaporation of an exothermically formed sodium oxide.

Acknowledgements

P.W.D. thanks the Science Research Council for the award of a Research Studentship. We are grateful to K.A. Prior for running the epitaxial structure-fit computer programme.

References

[1] P.J. Goddard and R.M. Lambert, Surface Sci. 51 (1975) 270.
[2] P.J. Goddard, K. Schwaha and R.M. Lambert, Surface Sci. 71 (1978) 351.
[3] G. Rovida and F. Pratesi, Surface Sci. 51 (1975) 270.
[4] E. Zanazzi, F. Jona, D.W. Jepsen and P.M. Marcus, Phys. Rev. B14 (1976) 432.
[5] G. Rovida, F. Pratesi, M. Maglietta and E. Ferroni, Japan. J. Appl. Phys. Suppl. 2(II) (1974) 117.
[6] E. Bertel, K. Schwaha and F.P. Netzer, Surface Sci. 83 (1979) 439.
[7] W. Erley and H. Wagner, Surface Sci. 66 (1977) 371.
[8] J.W. Gadzuk, J.K. Hartman and T.N. Rhodin, Phys. Rev. B4 (1971) 241.
[9] L.M. Kahn and S.C. Ying, Surface Sci. 59 (1976) 333.
[10] N.D. Lang, Solid State Commun. 9 (1971) 1015.
[11] N.D. Lang, Phys. Rev. B4 (1974) 12.
[12] F.J. Szalkowski and G.A. Somorjai, J. Chem. Phys. 56 (1972) 6097.
[13] F.J. Szalkowski and G.A. Somorjai, J. Chem. Phys. 61 (1974) 2064.
[14] F.J. Szalkowski and G.A. Somorjai, J. Chem. Phys. 64 (1976) 2985.
[15] P.W. Davies and R.M. Lambert, in preparation.
[16] P.W. Davies and R.M. Lambert, Surface Sci., submitted.
[17] S.A. Schukarev, M.A. Oranskaye, T.A. Tolmacheva, Y.S. Il'inskii, Russ. J. Inorg. Chem. (Engl. Transl.) 5 (1960) 3.
[18] R. Wyckoff, Crystal Structures, Vol. I (Wiley–Interscience, New York).
[19] R.E. McCarley, J.W. Roddy and K.O. Berry, Inorg. Chem. 3 (1964) 50.
[20] C.G. Goymour and D.A. King, JCS Faraday I, 69 (1973) 736, 749.
[21] D.L. Adams, Surface Sci. 42 (1974) 12.
[22] J.K. Roberts, Some Problems in Adsorption (Cambridge Univ. Press, 1939).
[23] M. Kitson and R.M. Lambert, in preparation.